

Supporting Information

Synergy of Experimental and Computational Chemistry: Structure and Biological Activity of Zn(II) Hydrazone Complexes

Milica Savić,^a Andrej Pevec,^b Nevena Stevanović,^c Irena Novaković,^a Ivana Z. Matić,^d Nina Petrović,^{d,e} Tatjana Stanojković,^d Karla Milčić,^c Matija Zlatar,^a Iztok Turel,^b Božidar Čobeljić,^c Miloš Milčić^{*c} and Maja Gruden^{*c}

^a University of Belgrade - Institute of chemistry, technology and metallurgy Department of chemistry, Njegoševa 12, P.O. Box 815, 11001 Belgrade, Serbia.

^b Faculty of Chemistry and Chemical Technology, University of Ljubljana Večna pot 113, 1000 Ljubljana, Slovenia.

^c University of Belgrade - Faculty of Chemistry Studentski trg 12–16, 11000 Belgrade, Serbia.

^d Institute for Oncology and Radiology of Serbia, Pasterova 14, 11000 Belgrade, Serbia.

^e "VINČA" Institute of Nuclear Sciences-National Institute of the Republic of Serbia, University of Belgrade, Belgrade 11000, Serbia.

Table of contents:

Figure S1. UV spectrum of Zn(II) complexes **1–3** at a concentration of 10⁻⁴ M in water.

Figure S2. UV spectrum of Zn(II) complexes **1–3** at a concentration of 10⁻⁴ M in DMSO.

Figure S3. UV spectrum of Zn(II) complexes **1–3** at a concentration of 10⁻⁴ M in methanol.

Figure S4. IR spectrum of **HLCl** ligand (*E*)-2-(2-(1-(6-bromopyridin-2-yl)ethylidene)hydrazinyl)-*N,N,N*-trimethyl-2-oxoethan-1-aminium chloride.

Figure S5. IR spectrum of complex **1** [ZnL₂](BF₄)₂.

Figure S6. IR spectrum of complex **2** [ZnL(OCN)₂].

Figure S7. IR spectrum of complex **3** [ZnL(N₃)₂].

Figure S8. ¹H NMR spectrum of **HLCl** ligand.

Figure S9. ¹³C NMR spectrum of **HLCl** ligand.

Figure S10. ¹H NMR spectrum of complex **1**.

Figure S11. ¹³C NMR spectrum of complex **1**.

Figure S12. ¹H NMR spectrum of complex **2**.

Figure S13. ¹³C NMR spectrum of complex **2**.

Figure S14. ¹H NMR spectrum of complex **3**.

Figure S15. ¹³C NMR spectrum of complex **3**.

Figure S16. Dual descriptor of the Fukui function for **HL** and complexes **1–3**.

Figure S17. Pauli and orbital deformation densities of complexes **1–3**.

Figure S18. Interaction of investigated complexes with **CYP51** enzyme.

Figure S19. Overlap of AlphaFold2 and Swiss model of **SQS** enzyme.

Figure S20. Interaction of investigated complexes with **SQS** enzyme.

Figure S21. Interaction of investigated complexes with **HMG-CoA** transferase, **SMT** and **SQE** enzymes.

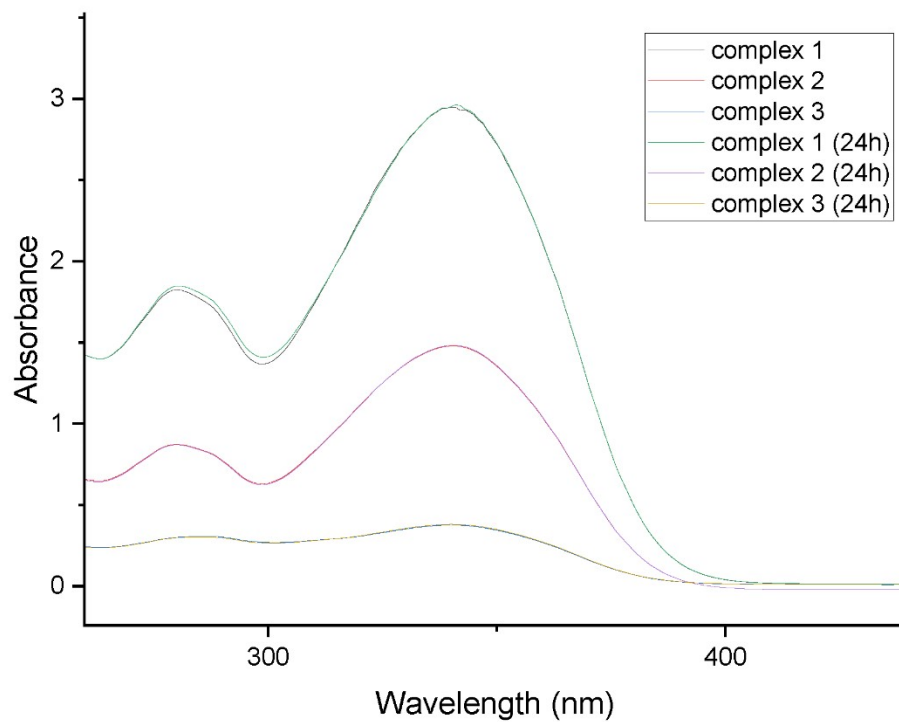


Figure S1. UV spectrum of Zn(II) complexes **1–3** at a concentration of 10^{-4} M in water.

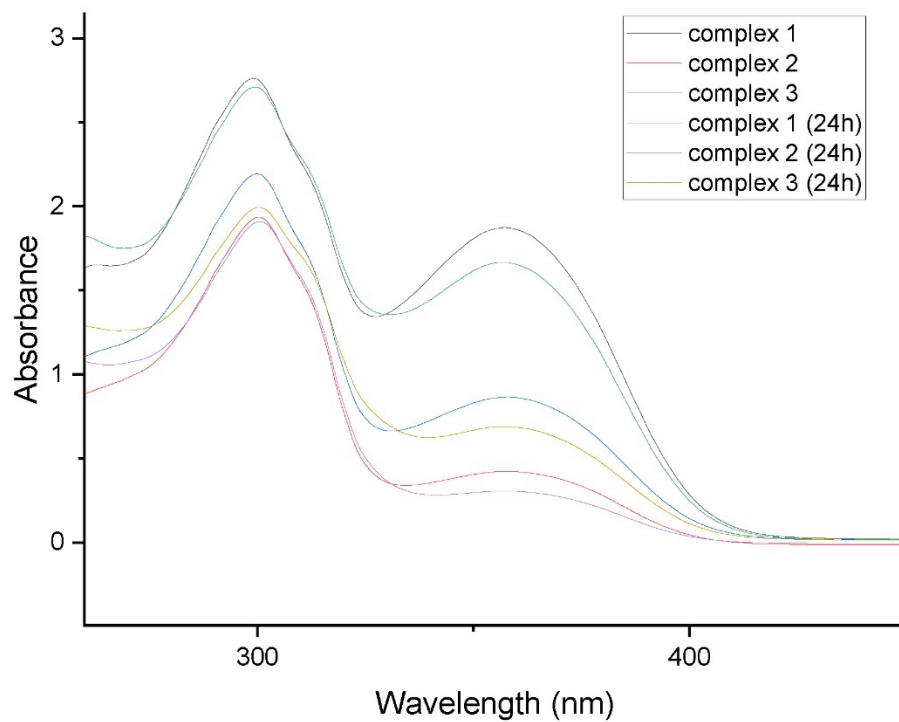


Figure S2. UV spectrum of Zn(II) complexes **1–3** at a concentration of 10^{-4} M in DMSO.

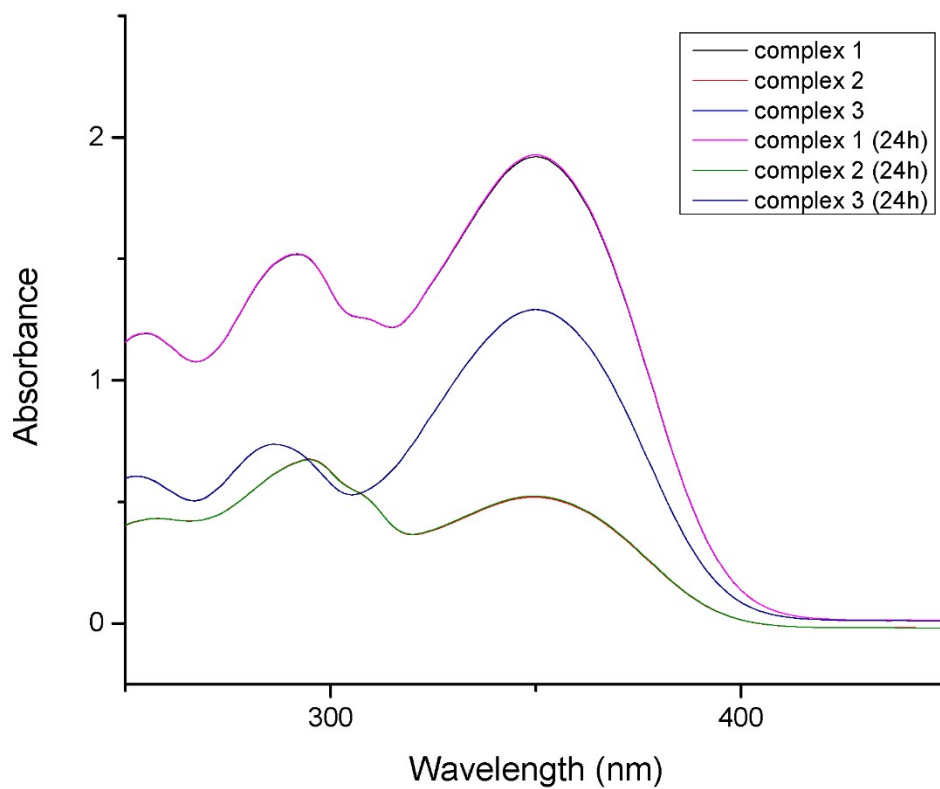


Figure S3. UV spectrum of Zn(II) complexes **1–3** at a concentration of 10^{-4} M in methanol.

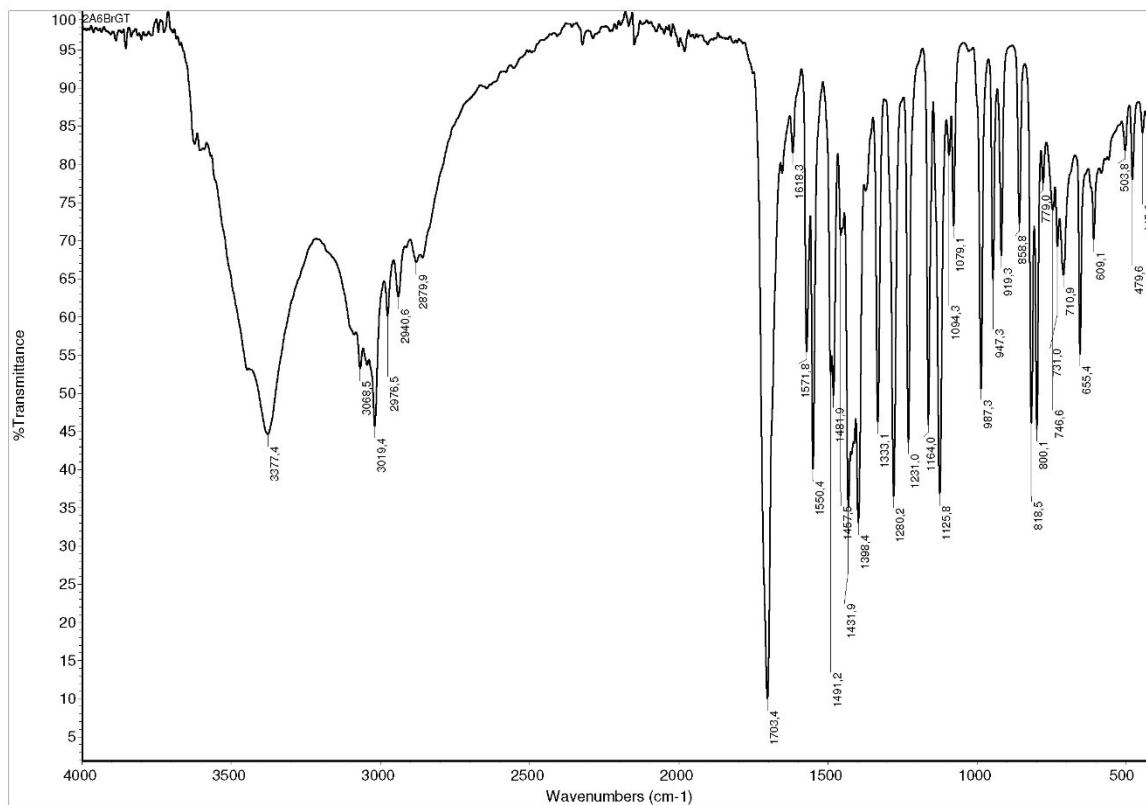


Figure S4. IR spectrum of HLCI ligand.

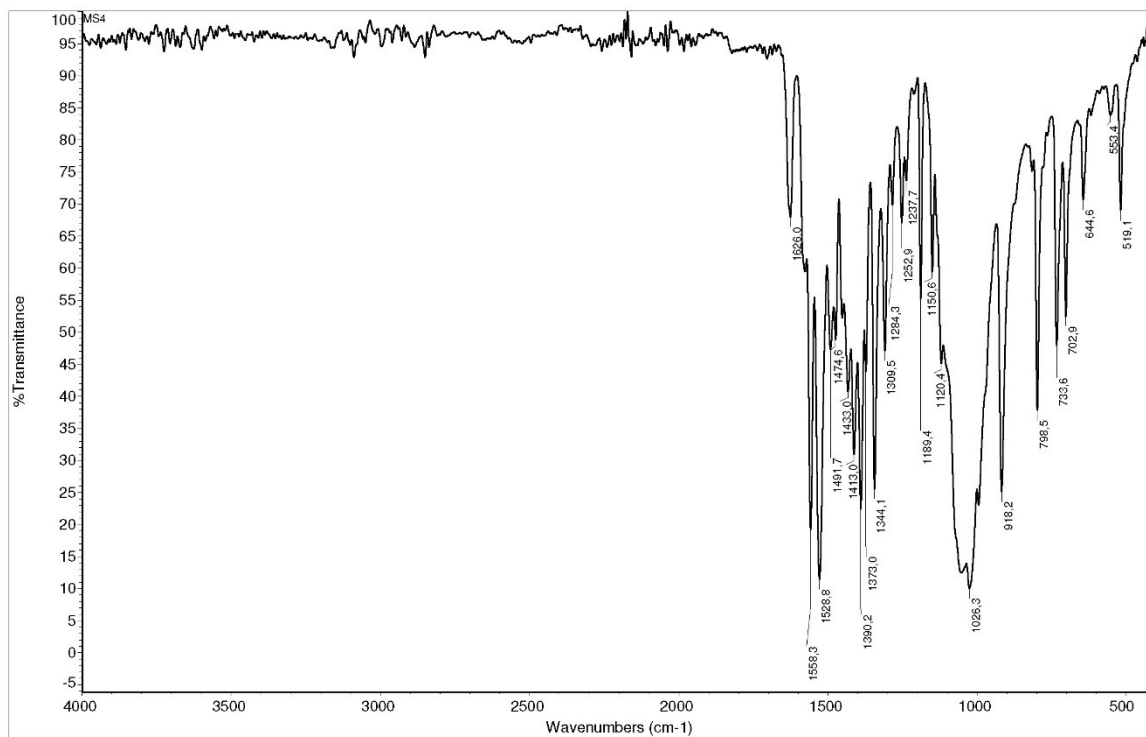


Figure S5. IR spectrum of complex 1.

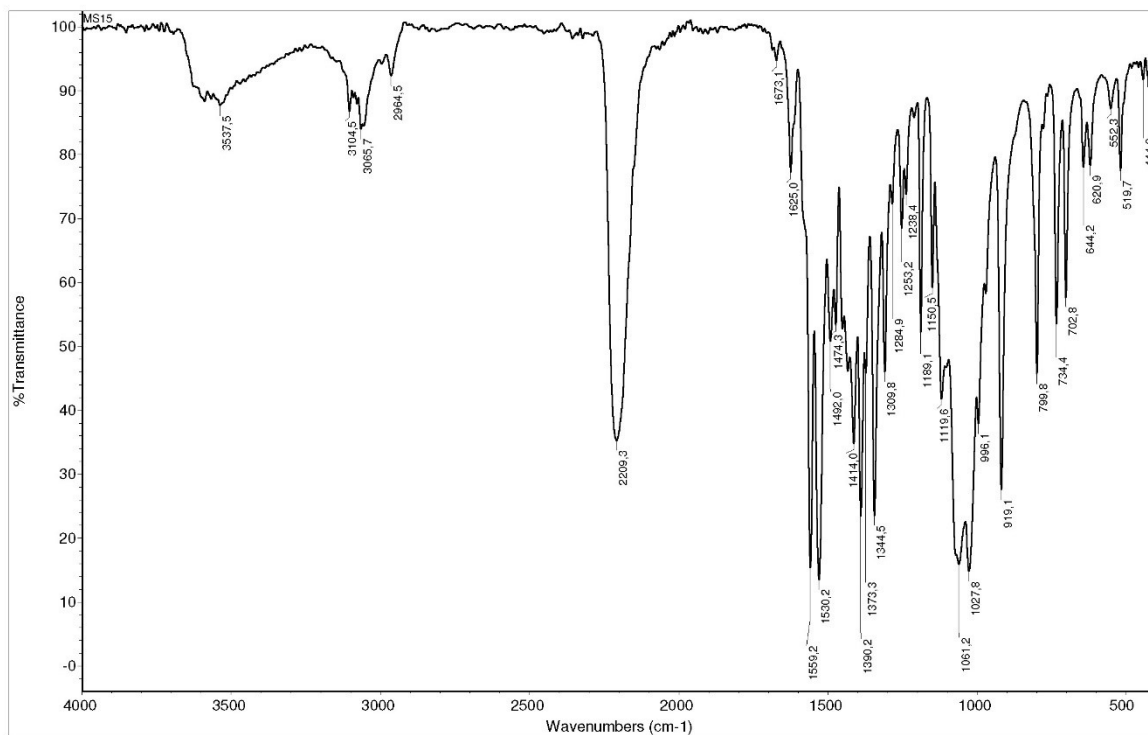


Figure S6. IR spectrum of complex 2.

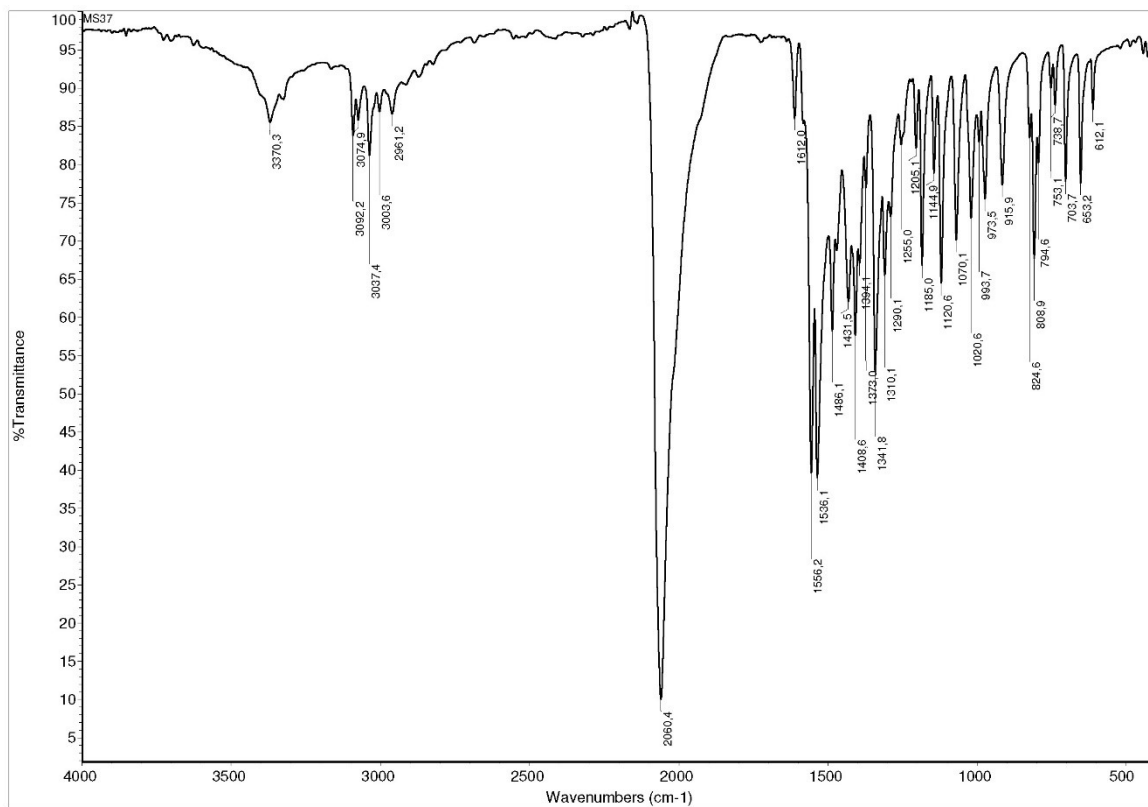


Figure S7. IR spectrum of complex 3.

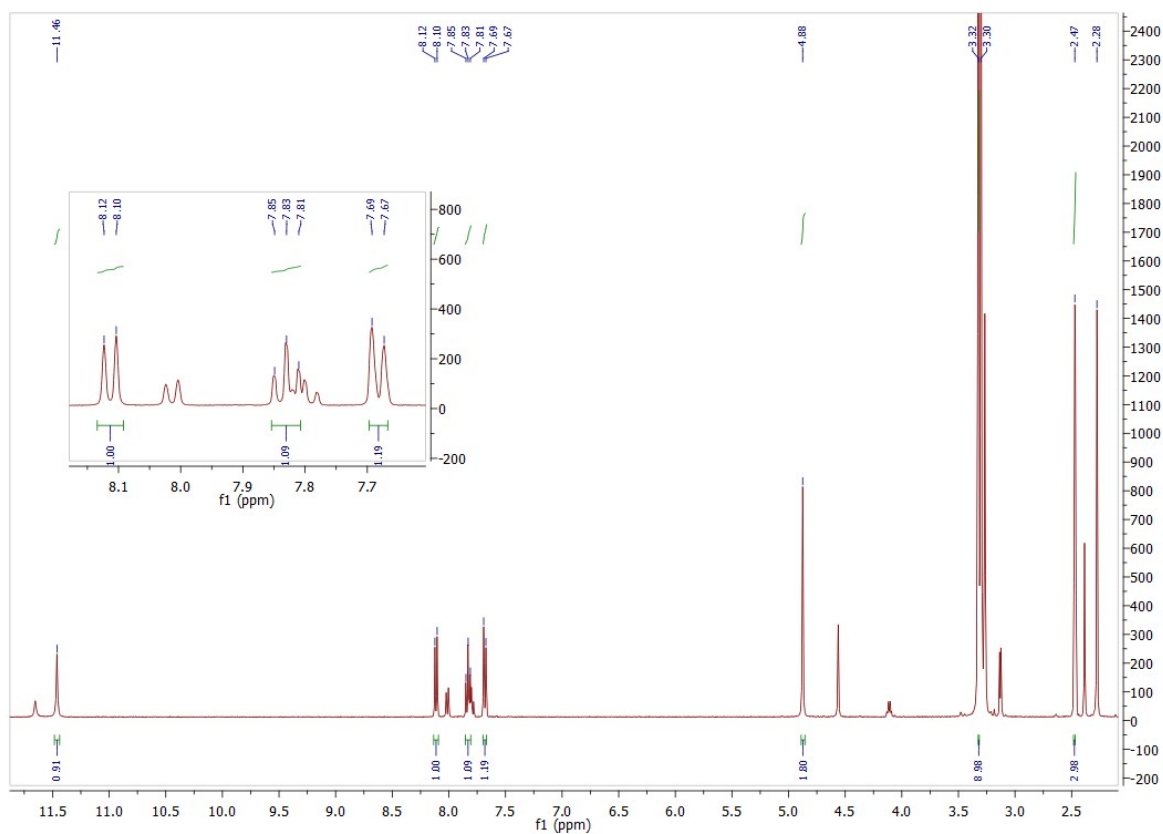


Figure S8. ^1H NMR spectrum of HLCI ligand.

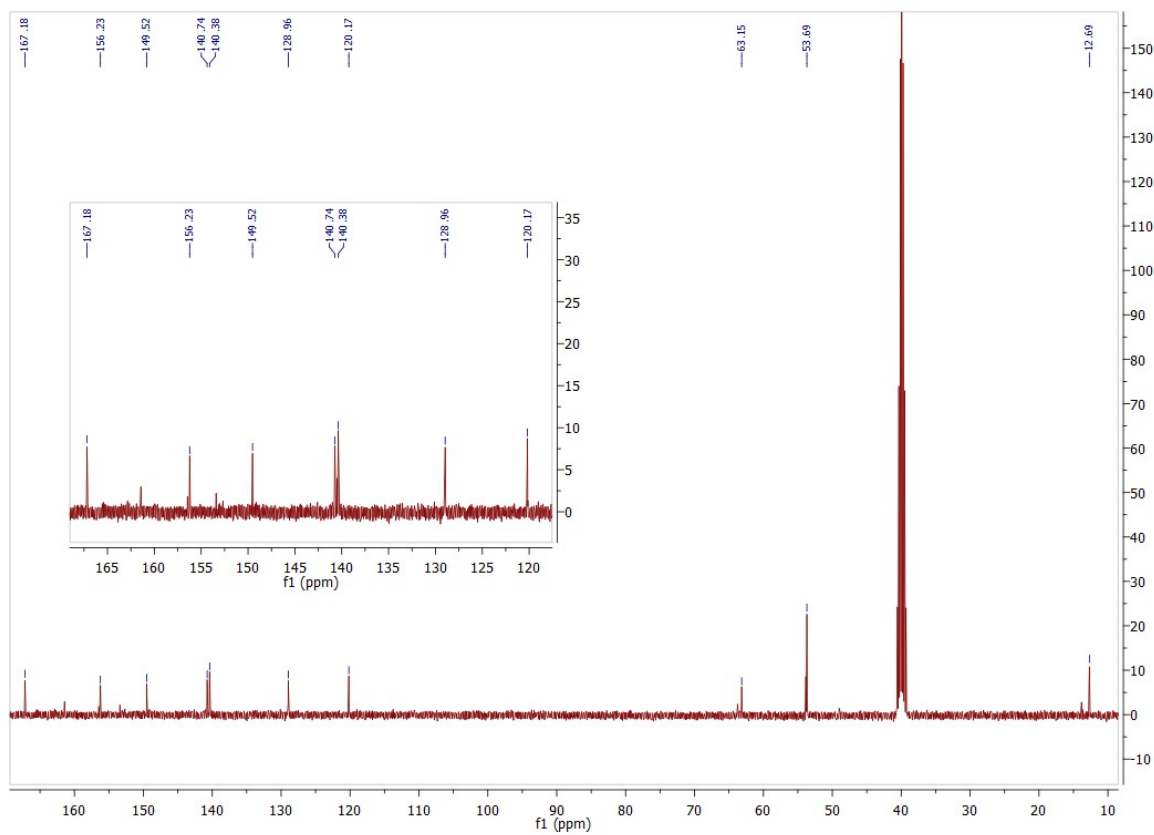


Figure S9. ^{13}C NMR spectrum of HLCI ligand.

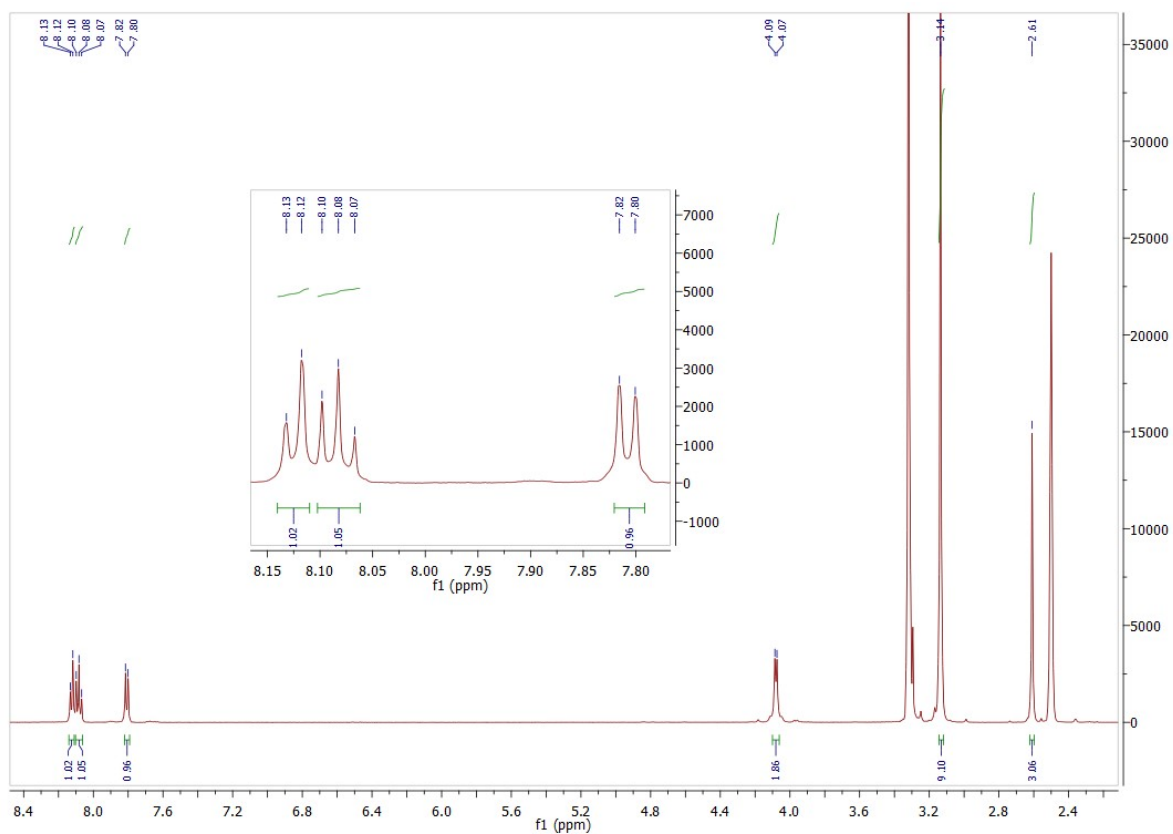


Figure S10. ^1H NMR spectrum of complex 1.

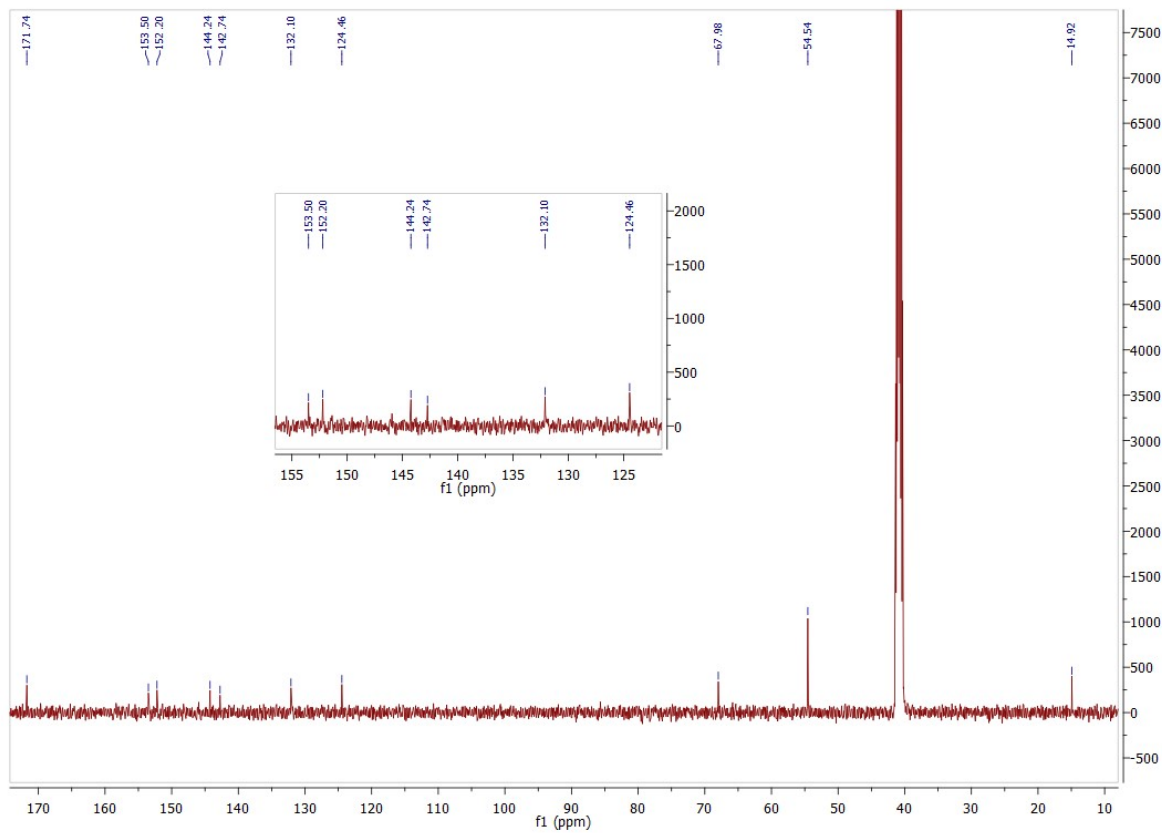


Figure S11. ^{13}C NMR spectrum of complex 1.

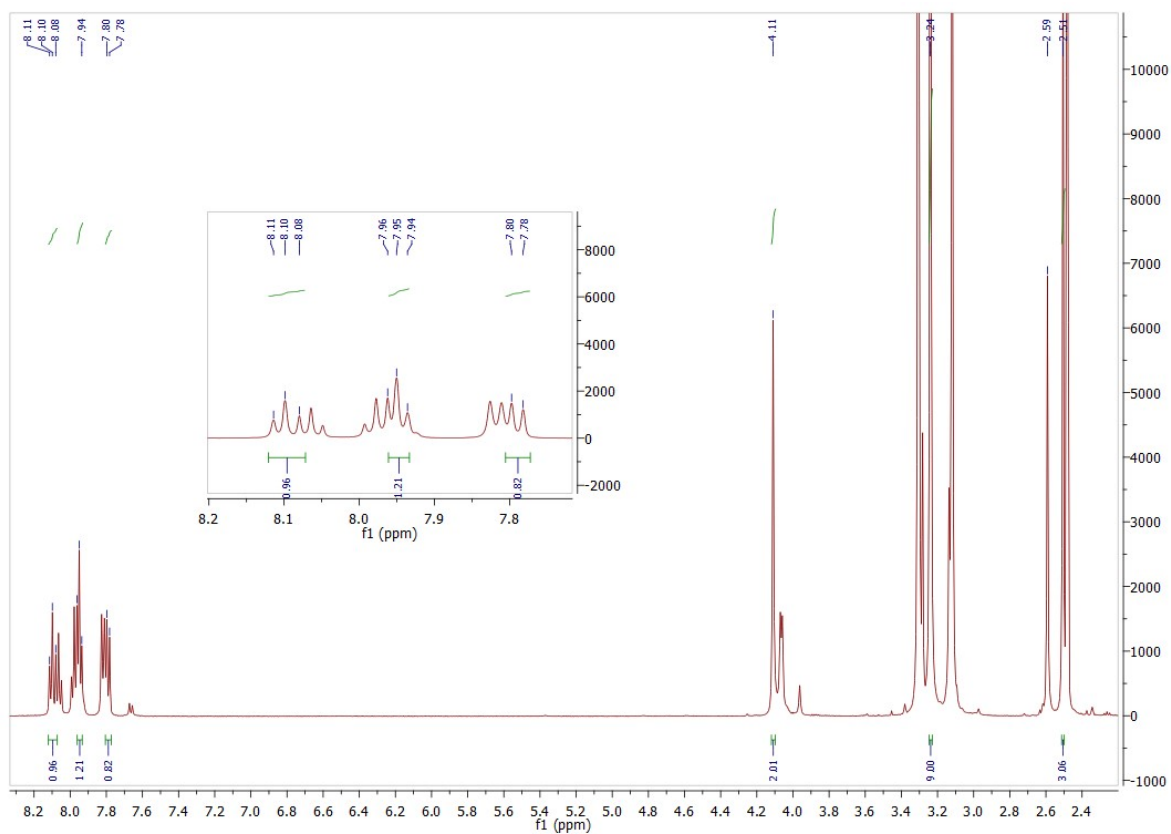


Figure S12. ^1H NMR spectrum of complex 2.

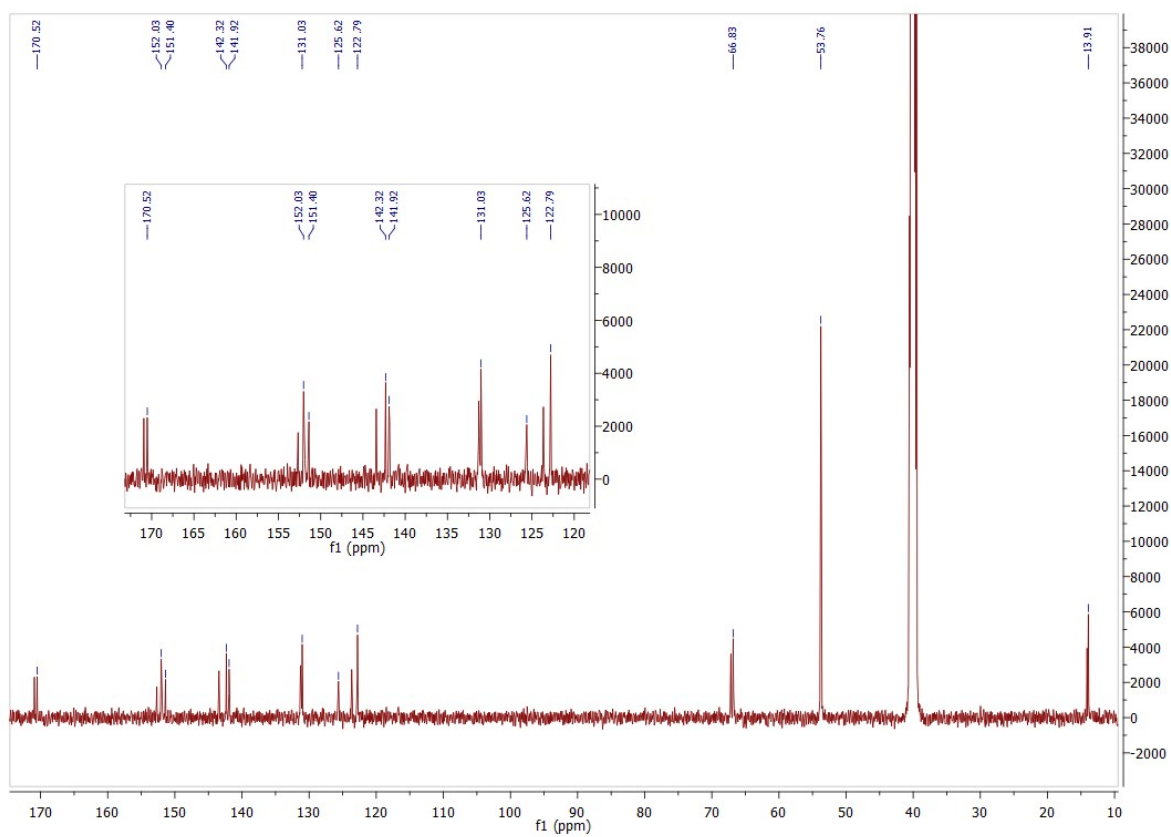


Figure S13. ^{13}C NMR spectrum of complex 2.

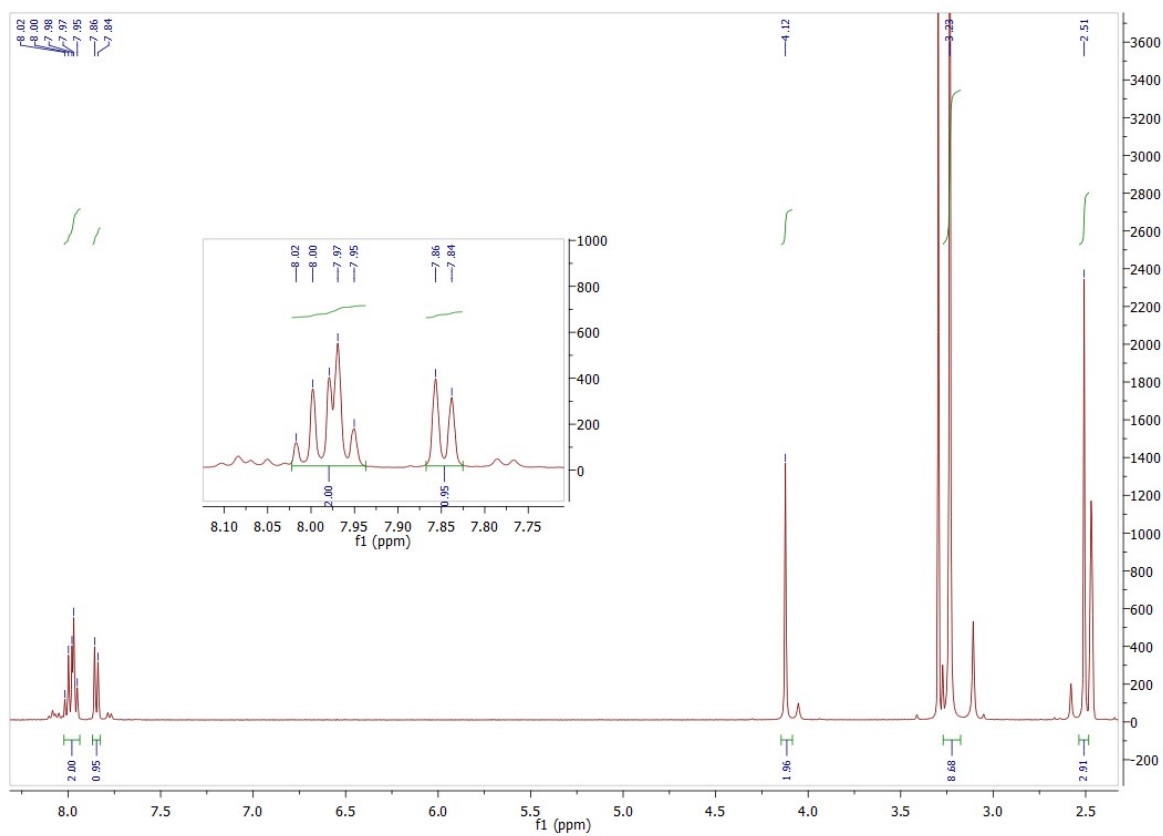


Figure S14. ^1H NMR spectrum of complex 3.

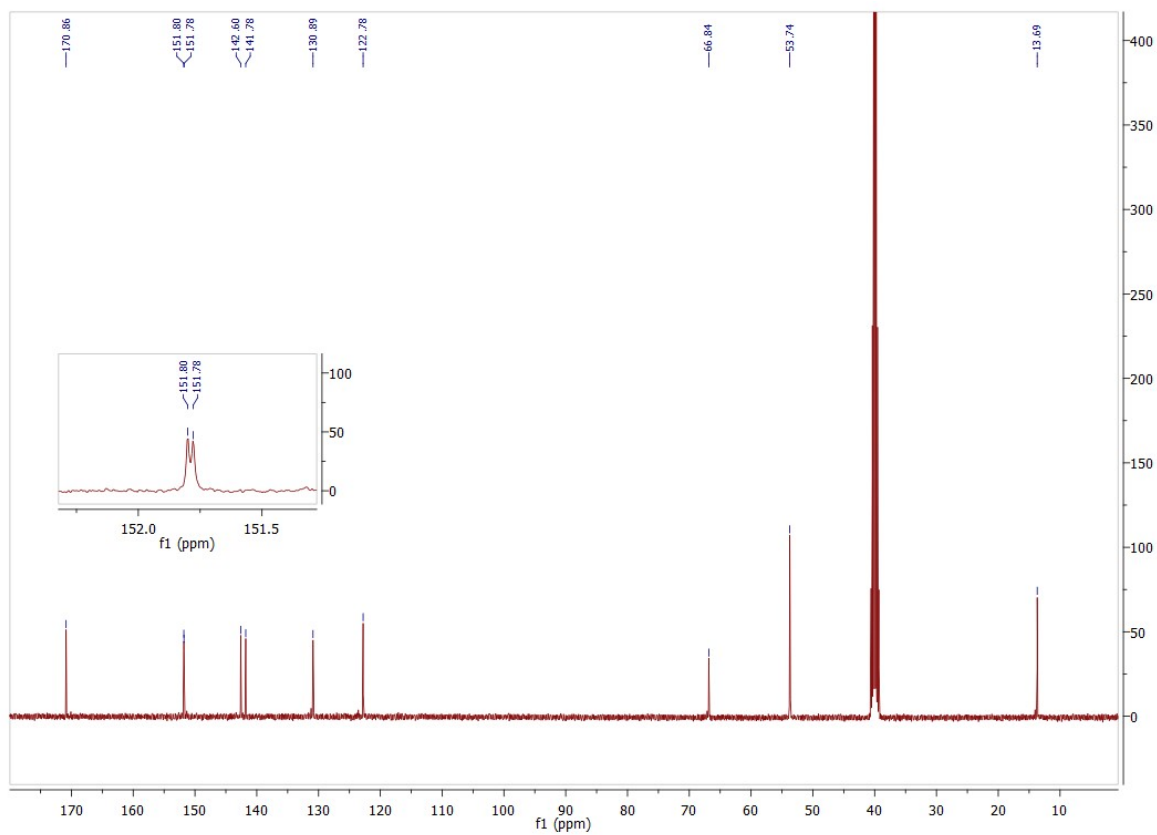


Figure S15. ^{13}C NMR spectrum of complex 3.

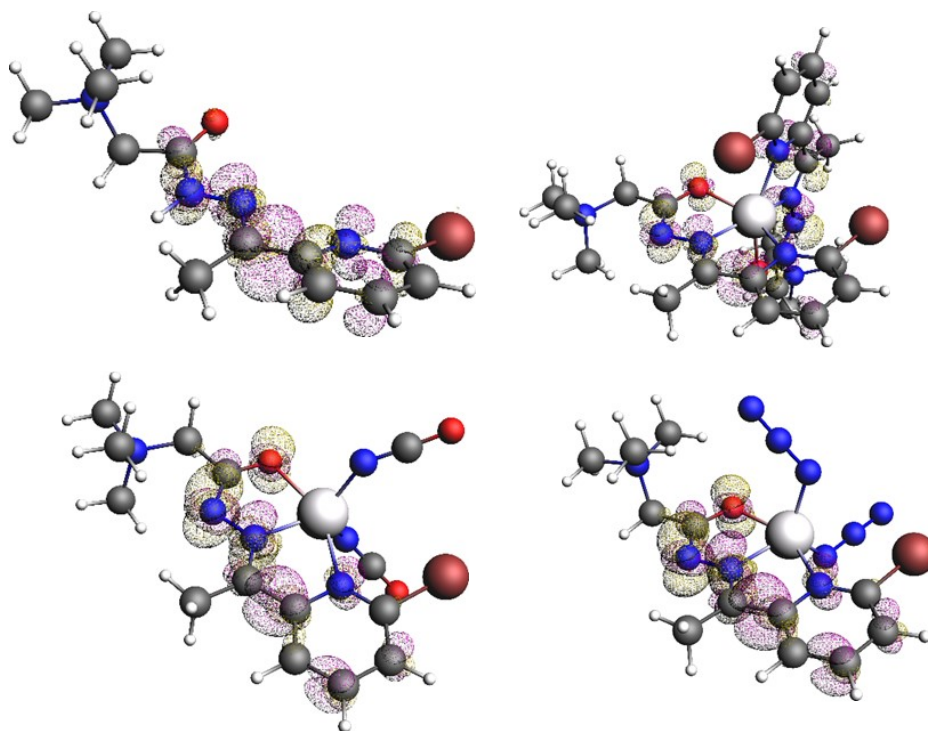


Figure S16. Dual descriptor of the Fukui function (isosurfaces 0.003 au), calculated at ZORA-CAM-B3LYP/TZP-COSMO (water)//ZORA-BP86-D4/TZP-COSMO(water) level of theory of ligand HL^+ and complex **1** (up row) and complexes **2** and **3** (down). Positive values are shown in yellow, and negative values in purple.

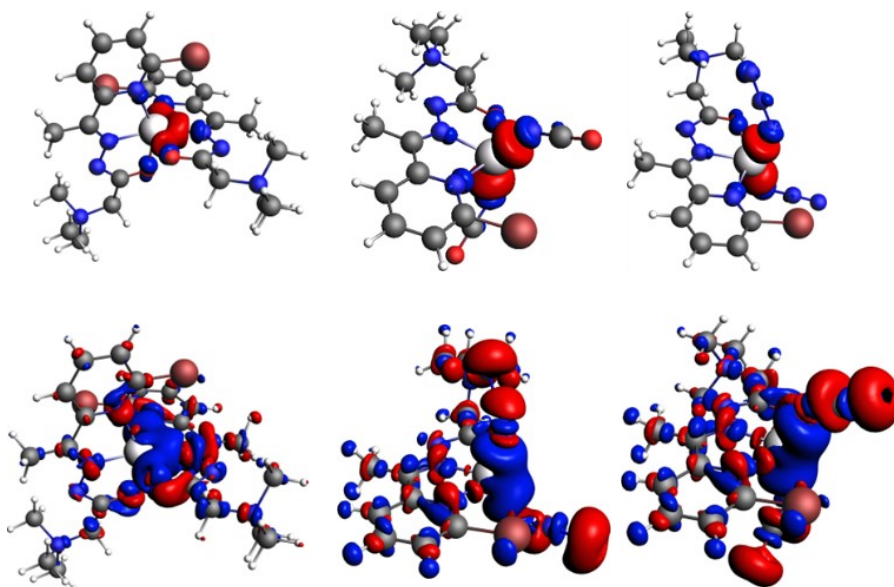


Figure S17. Pauli deformation densities (up row, isosurfaces 0.003 au), and orbital deformation densities (down, isosurfaces 0.003 au) calculated ZORA-BP86-D4/TZP level of theory of complexes **1–3** (down). Density depletion in red; density accumulation in blue.

Complexes **2** and **3** bind in the active site of CYP51 (**Figure S18. A**), interacting with HEM group via π - π T shaped interactions (**Figure S18, B and C**). Complex **1** is too large to fit in CYP51 active site and the best binding pose for this complex is outside of the active site at the surface of the protein (**Figure S18. A**).

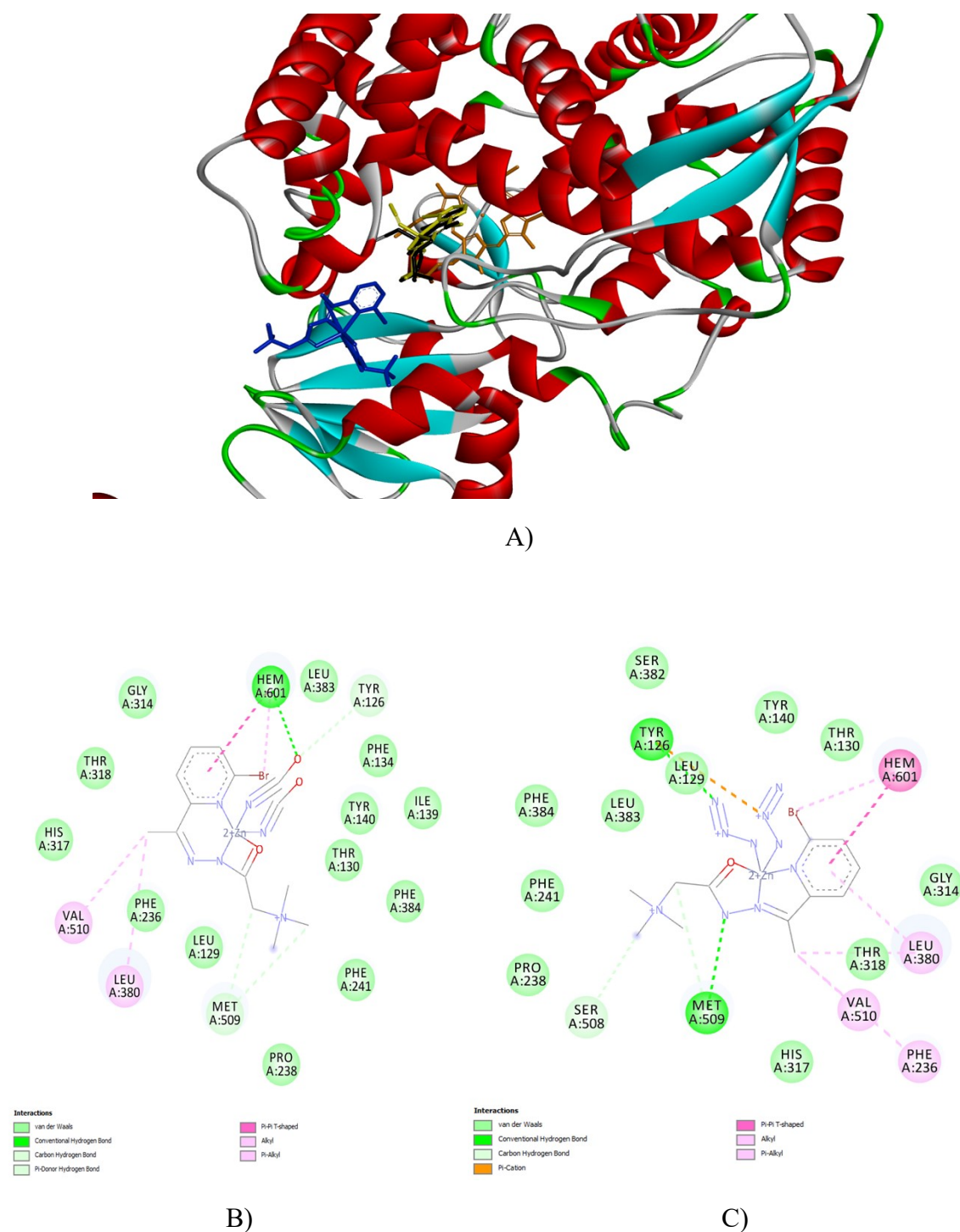


Figure S18. A) The best binding poses for investigated complexes with CYP51 enzyme found by docking study. Complex **1** (blue sticks) binds at the protein surface, while complexes **2** (black sticks) and **3** (yellow sticks) bind inside the active site. HEM group is shown with orange stick representation. B) and C) 2D interaction diagrams for complexes **2** and **3** with amino acids from CYP51 active site.

SQS enzyme is modeled with two different homology modeling techniques Swiss model¹ and AlphaFold2². Template for Swiss model was crystal structure of squalene synthase from *Aspergillus flavus* (PDBID: 7wgh) and for AlphaFold2 model templates were crystal structures of human squalene synthase (PDBIDs: 3wcc and 3wca) and squalene synthase from *Trypanosoma cruzi*. The alignment of two modeled structures is shown on **Figure S19**. AlphaFold2 model contains all 444 amino acids while in Swiss model 33 amino acids from N-terminus and 62 amino acids from C-terminus are omitted. Since there is good overlap of the two models in the active site area (**Figure S19**.) the results of the docking study are very similar for both models.

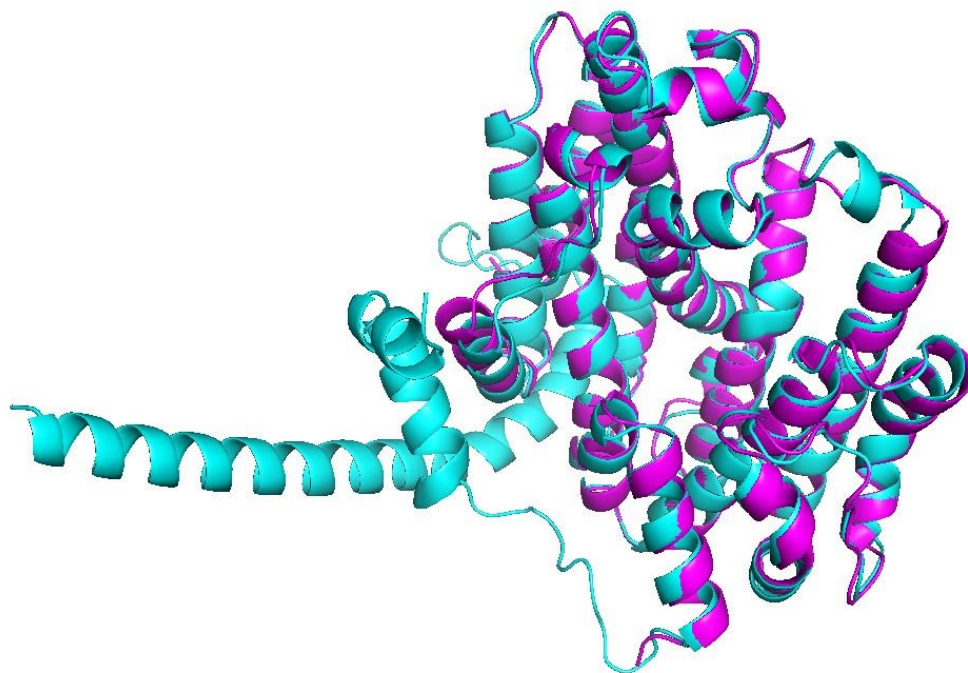


Figure S19. Overlap of AlphaFold2 model (cyan) and Swiss model (magenta) structures of SQS enzyme. (Image created with PyMol³ software)

The best binding pose for complex **3** is in the middle of active site, and for the complex **2** at the edge of the SQS active site (**Figure S20. A**). Complex **1** does not bind at the active site, the best binding pose is located at the protein surface (**Figure S20. A**). The main interactions between complex **2** and active site amino acids are hydrogen bond and cation- π (**Figure S20. B**), while for the complex **3** π - π T shaped and σ - π interactions are also found (**Figure S20. C**).

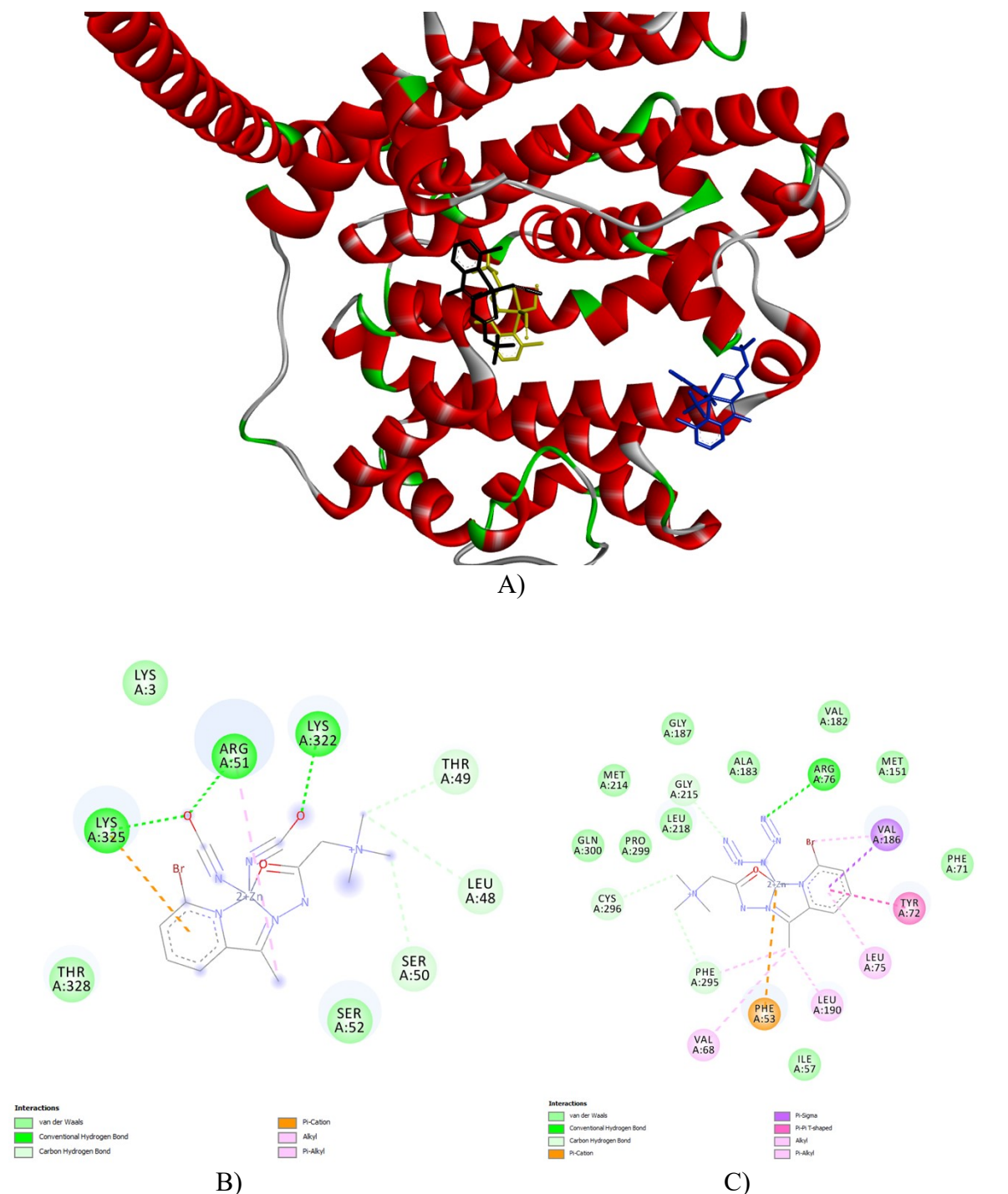


Figure S20. A) The best binding poses for complex **1** (blue sticks), complex **2** (black sticks) and complex **3** (yellow sticks) with SQS enzyme found by docking study. 2D interactions diagram between B) complex **2** and C) complex **3** and amino acids from SQS active site.

HMG-CoA transferase, SMT and SQE enzymes have narrow active sites that cannot accommodate large molecules of investigated complex. Docking studies of these proteins (both models) produced only poses with interactions with amino acids from protein surface (**Figure S21**).

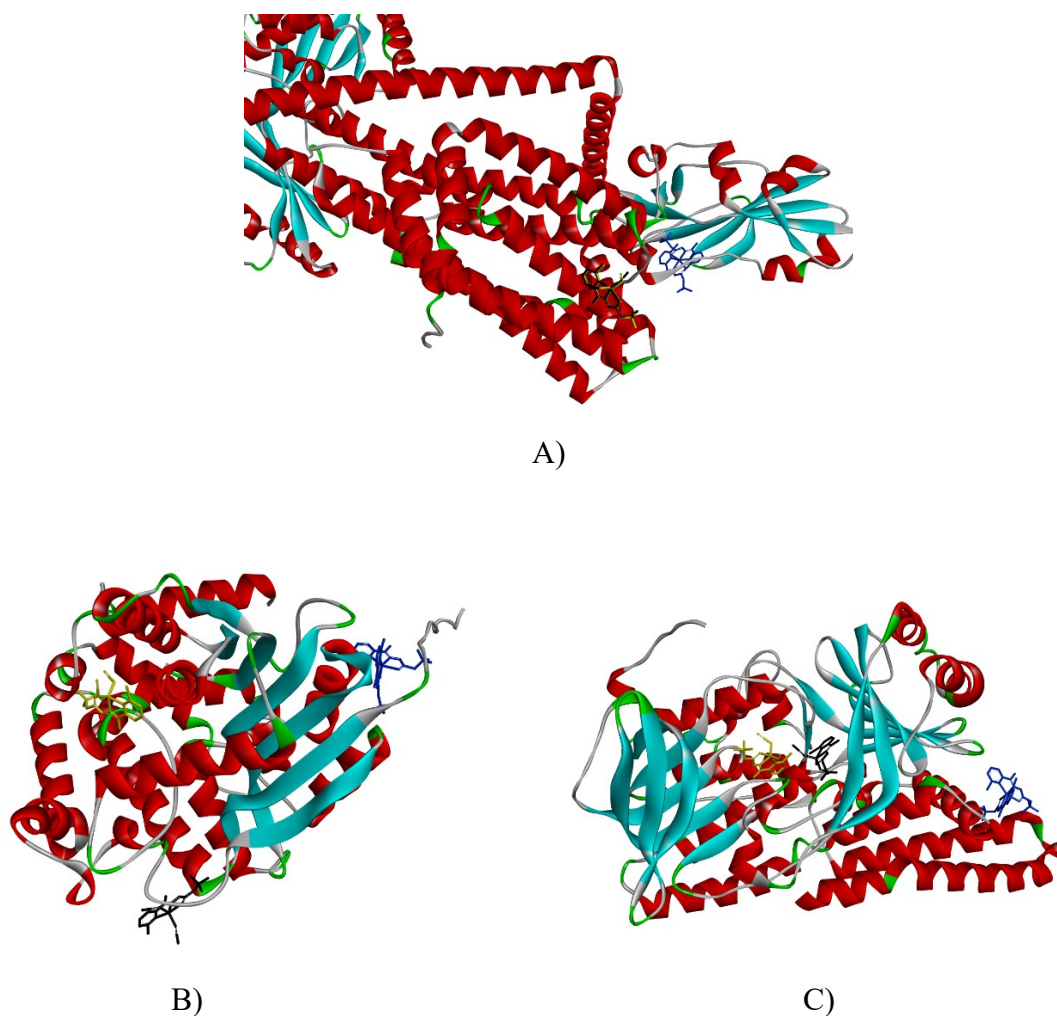


Figure S21. Best binding poses of investigated complexes found by the docking study for A) HMG-CoA transferase, B) SMT and C) SQE enzymes. Color code: blue sticks – complex 1, black sticks – complex 2, yellow sticks – complex 3.

Literature:

- 1 S. Bienert, A. Waterhouse, T. A. P. de Beer, G. Tauriello, G. Studer, L. Bordoli and T. Schwede, *Nucleic Acids Res*, 2017, **45**, D313–D319.
- 2 J. Jumper, R. Evans, A. Pritzel, T. Green, M. Figurnov, O. Ronneberger, K. Tunyasuvunakool, R. Bates, A. Židek, A. Potapenko, A. Bridgland, C. Meyer, S. A. A. Kohl, A. J. Ballard, A. Cowie, B. Romera-Paredes, S. Nikolov, R. Jain, J. Adler, T. Back, S. Petersen, D. Reiman, E. Clancy, M. Zielinski, M. Steinegger, M. Pacholska, T. Berghammer, S. Bodenstein, D. Silver, O. Vinyals, A. W. Senior, K. Kavukcuoglu, P. Kohli and D. Hassabis, *Nature*, 2021, **596**, 583–589.
- 3 The PyMOL Molecular Graphics System, Version 3.0 Schrödinger, LLC.